Engineering Notes

Unsteady Reynolds-Averaged Navier–Stokes-Based Hybrid Methodologies for Rotor–Fuselage Interaction

Eliot W. Quon* and Marilyn J. Smith[†]
*Georgia Institute of Technology,
Atlanta, Georgia 30332-0150*
and
Glen R. Whitehouse[‡] and Dan Wachspress[§]
Continuum Dynamics, Inc., Ewing, New Jersey 08618-2302

I. Introduction

LIFTING bodies produce wakes that interact with other bodies immersed in the same fluid. In particular for rotorcraft, the problem becomes significantly more complicated since the rotor wake remains near the vehicle in hover, descent, and low-speed forward flight. The proximity of the wake alters the inflow distribution at the rotor and modifies the helicopter thrust. Moreover, since the main rotor wake may impinge on the fuselage, such interactions are an important consideration in modern rotorcraft design. For example, empennage impingement may result in undesirable handling qualities such as low-speed pitchup and tail buffet. Moreover, the wake can also generate unsteady impulsive loads on the fuselage, resulting in vibrations, thus negatively impacting the crew and passenger flight experience. Given the complexity of rotorcraft interactional aerodynamics problems, it is common for tail and empennage designs to be modified significantly after first flight [1].

Development of many aerospace technologies, not limited to helicopter rotor–fuselage applications, requires accurate resolution of both near- and far-field flow phenomena. Numerical prediction of wakes involve a tradeoff between accuracy, turnaround time, and computational expense [2]. Current grid-based computational fluid dynamics (CFD) codes can theoretically model the entire flowfield, but resolution and preservation of wake features become difficult since typical grid sizes used in industrial simulations are susceptible to numerical dissipation. The artificial diffusion of vorticity that results can be mitigated using grid adaptation techniques and higher-order methods [2–4], but this may not be practical for all applications since computational cost increases significantly. For this reason, computationally efficient hybrid methods may be more attractive, especially during design and for flight-test support.

*Ph.D. Candidate, Daniel Guggenheim School of Aerospace Engineering. Student Member AIAA.
[†]Associate Professor, Daniel Guggenheim School of Aerospace Engineering. Associate Fellow AIAA.
[‡]Associate. Senior Member AIAA.
[§]Senior Associate.

Traditional Lagrangian free-wake methods are inexpensive but become less accurate when vortex elements in the wake become distorted and tangled due to interactions with other vortices and solid bodies (i.e., rotor blades and the fuselage) [5]. These interactions typically occur in the rotor near field, which motivates coupling to a CFD solver to resolve the highly viscous and possibly compressible flow near the rotor. In such an approach, the CFD code does not have to resolve the entire wake region; thus, the size of the CFD domain can be greatly reduced and computational efficiency maximized. Additional challenges associated with surface interactions arise when modeling problems such as rotor–fuselage interactions.

The ability of two approaches to hybridize a Reynolds-averaged Navier–Stokes (RANS) CFD solver and a free-wake method for the rotor–fuselage interaction problem is investigated. Predictions are compared with experimental data, as well as prior numerical predictions made with individual code simulations.

II. Computational Methodologies

Continuum Dynamics, Inc.'s, comprehensive rotorcraft code, CHARM, has been used successfully to model rotorcraft airloads and blade–vortex interaction noise. CHARM is equipped with lifting surface blade aerodynamics and a full-span free-vortex wake model that directly computes the rollup of the wake sheet into concentrated vortices. The free-wake model does not dissipate vorticity and provides rapid turnaround, while surface pressures can be determined with an integrated panel method [5]. FUN3D [6], a fully unstructured Navier–Stokes RANS solver developed primarily by researchers at NASA, includes overset and adaptive mesh capabilities to enable accurate resolution of multiple frames of motion, making it suitable for rotorcraft analysis.

An interface between FUN3D and CHARM, derived from prior efforts [7,8], has been developed to perform fully coupled time-accurate calculations. The FUN3D near-body solution is used to determine the local flowfield at each time step, which is used to determine an equivalent blade loading for the CHARM wake module to update the strength and position of vortex filaments. After the wake solution is advanced, induced velocities are calculated and their influence is imposed on the outer boundary of the FUN3D domain through a modified far-field boundary condition. The FUN3D solution is then advanced to the next time step, and the coupling cycle repeats. A detailed discussion of boundary conditions and coupling strategy is further detailed in [7–9].

III. Results

Rotor–fuselage interactions were investigated by Elliot et al. [10], Mineck and Althoff Gorton [11], and Freeman and Mineck [12] at NASA Langley Research Center using a generic fuselage configuration (rotor–body interaction, or ROBIN, model). The ROBIN fuselage geometry is defined by a set of algebraic equations at various fuselage stations to yield a streamlined slender fuselage body and an engine mount (doghouse). Wind-tunnel tests were performed with and without a four-bladed rectangular-planform rotor with a solidity of $\sigma = 0.098$. The 33.88 in. blades comprised a NACA 0012 section with a 2.7 in. chord and a -8 deg linear twist. The tests are summarized in the recent paper by Smith et al. [13], including data corrections and trim conditions for FUN3D that were applied in these simulations. Pressures from the ROBIN experiments were documented as modified pressure coefficients, defined as $C'_p = \{(p - p_{\mathrm{avg}})/[0.5\rho(\Omega R)^2]\} \times 100$, where the difference in local and mean pressures was nondimensionalized by the density ρ and the square of the rotor tip speed ΩR. To facilitate the analysis and comparison of

the unsteady data, a shift of 252 deg was added to account for experimental phase lag [14].

A. Accuracy of Isolated Fuselage Predictions

CHARM predictions of the isolated fuselage using 2174 panels are compared with the experimental data [12] and FUN3D predictions [13] in Fig. 1. Both sets of predictions are generally very good up to 18% of the nondimensional fuselage length ($x/\ell = 0.35$, where ℓ is the fuselage half-length and x is referenced from the nose). At $x/\ell = 0.47$ and locations aft, CHARM and FUN3D predict pressures that vary little around the fuselage, as one would expect for the nonlifting streamlined symmetrical body. Slight differences from the experiment occur, as neither the fuselage strut nor the hub from the experiment were modeled [13]. At $x/\ell = 0.47$, there is flow separation at $z/\ell > 0.125$ (on the doghouse) predicted by FUN3D that, as expected from inviscid theory, is not predicted by CHARM.

B. Standalone Solver Results

Unsteady pressure predictions for the solvers run individually are compared in Fig. 2 for an advance ratio of $\mu = 0.15$ and thrust $C_T = 0.0064$. Correlations were made for the top centerline of the fuselage at $x/\ell = 0.2$, 0.9, 1.18, and 1.56 locations. CHARM predictions were performed with 24 azimuthal increments, 16 spanwise filaments, and a total of seven turns of wake (three turns of full span followed by four turns of tip and root filaments). Calculations were trimmed for 20 revolutions. With the converged controls held fixed, each calculation was run for an additional 20 revolutions, over which the predicted pressures were averaged.

The FUN3D reference solution was obtained using four 2.3 million node blade grids on a 5.1 million node background grid. The background includes the fuselage as well as the strut mounts from the actual experiment and extends 2.5 fuselage lengths in all directions. Details of the grid study performed for this setup are found in [13]. Trimming was performed over two revolutions, and an additional revolution was simulated to reach a steady-state solution.

Overall, it is observed that the CHARM predictions are consistent with previous predictions made with FUN3D and a vorticity transport method (VTM) that solves the Navier–Stokes equations in vorticity–velocity form [13,14], although at a fraction of the computational cost. All three analyses correlate closely with the experimental data in areas where viscous effects can be neglected. At $\mu = 0.15$ (Fig. 2), CHARM, VTM, and FUN3D are comparable with experimental data in terms of both phase and magnitude, except for a slight underprediction of magnitude at $x/\ell = 0.9$ and 1.18. It is believed that this discrepancy is due to bluff body shedding off the aft end of the doghouse and the hub on the top of the fuselage [14]. Similar trends were also observed at higher advance ratios [7,13,14] where predictions fore and aft of the doghouse are generally excellent but both analyses significantly underpredict the magnitude of the pressure pulses along the top of the doghouse.

C. Hybrid FUN3D/CHARM Approaches

Two different hybrid approaches were examined to investigate the variable fidelity methodology. These were once again evaluated on the ROBIN configuration at an advance ratio of $\mu = 0.15$ and thrust of $C_T = 0.0064$, for comparison with the standalone code predictions. The first approach coupled FUN3D and CHARM, where FUN3D was used to predict the blade airloads, and the CHARM wake panel module was used to predict the rotor wake and fuselage loads. Next, CHARM provided an estimate of the blade airloads and rotor wake, whereas FUN3D was employed to predict the unsteady viscous fuselage loading.

1. FUN3D Rotor Blades with CHARM Wake and Fuselage

FUN3D and the CHARM wake panel module were coupled together in a conventional hybrid arrangement where the FUN3D airloads and CHARM wake solutions influenced each other in a closed loop. In a first, to the authors' knowledge, for this type of hybrid arrangement, a fuselage was included in the calculation using CHARM's integral panel model. The viscous ROBIN blade grids
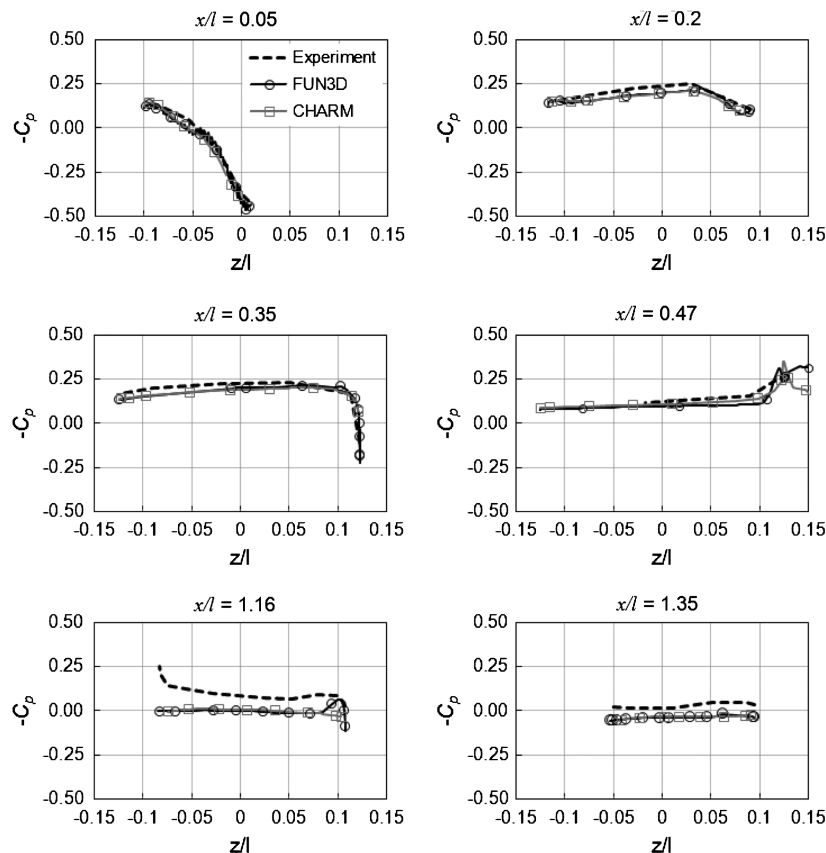

Fig. 1   Steady pressure on the isolated ROBIN fuselage at various locations.
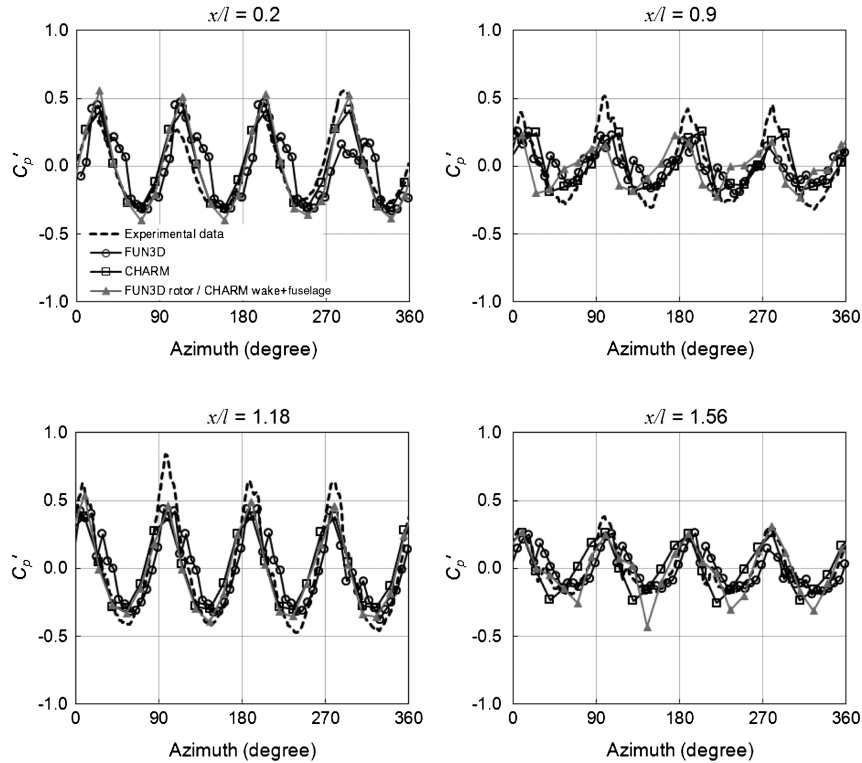
Fig. 2 Comparison of unsteady surface pressures along the top centerline of the ROBIN fuselage predicted with FUN3D, CHARM, and hybrid FUN3D/ CHARM (FUN3D rotor with CHARM wake and fuselage).

used in these studies contained 9.2 million nodes (four blades with near field grids of 2.31 million points). To model the cyclic motion present in the simulation, a small background grid centered about the rotor disk was generated. The extent of the grid was chosen to enclose the swept area of the rotor blade grids.

The complex FUN3D/CHARM wake structure for this simulation is illustrated in Fig. 3, where the interaction of the wake with the aft empennage is clearly apparent. In Fig. 3, the darker wake traces correspond to tip vorticity, while the lighter traces indicate root vorticity. Vectors bounding the rotor are also shown in these figures and represent the wake-induced velocity at each of the FUN3D nodes along the CFD boundary.

In Fig. 2, it is observed that, in general, all predictions show good reproduction of the magnitude and phase of the peaks in unsteady pressure. The modified flow predicted by the FUN3D/CHARM computations can be readily observed at this moderate advance ratio. Directly below the hub ($x/\ell = 0.9$), the predicted fuselage pressures

a) Orthogonal view

b) Side view

Fig. 3 Hybrid FUN3D/CHARM (FUN3D rotor coupled with CHARM wake and fuselage) wake predictions for the $\mu = 0.15$ ROBIN case.

have the highest disparity with the experiment due to the region of unsteady separated flow attributed to hub effects. Compression peaks predicted by FUN3D/CHARM are close to the high-resolution FUN3D predictions, but the suction peaks are closer to the CHARM solutions. The more accurate approximation at the compression peaks is due to the improvement in the rotor wake magnitudes captured by FUN3D. On the aft fuselage at $x/\ell = 1.18$ and $x/\ell = 1.56$, wake–fuselage interactions involving the combined influence of the rotor, doghouse, and hub wakes were observed in the individual FUN3D predictions [13], as denoted by the abrupt changes noted in the pressure rises. While these fluctuations were not apparent in the FUN3D/CHARM results, the hybrid predictions still provide the best overall correlation with experiment, suggesting the future potential of the hybrid methodology. Improved phase and character of the pressures can also be observed at $x/\ell = 1.56$, although the hybrid suction peaks tend to be overpredicted. The coupled FUN3D/CHARM approach more accurately predicts the slopes of the pressures (seen more clearly in Fig. 4) and appears to capture the higher harmonic feature in the unsteady pressures at about 30 deg. However, similar features at 120, 210, and 300 deg are not well captured by any of the three methods. Nevertheless, given the significant reduction in computational costs, the results are very promising.

The cost per revolution of performing this hybrid analysis is approximately half that of running a full FUN3D simulation, requiring 9.6 h per revolution compared with 17.1. Initially, two partial revolutions (where one partial revolution is 90 deg for a four-bladed rotor) were run with the minimal FUN3D configuration to eliminate transients from the CFD solution. Since 360 deg of periodic data can be composed from a partial revolution by copying the solution from each blade, a complete revolution of CFD blade loadings from the second partial revolution can be used to initialize the CHARM free-wake solution. Afterward, three fully coupled revolutions were run, with information exchanged at 1 deg azimuthal intervals. The final hybrid periodic solution was obtained by averaging over the last four partial revolutions at a total cost of 2150 CPU hours, compared with 3260 CPU hours when running FUN3D alone.
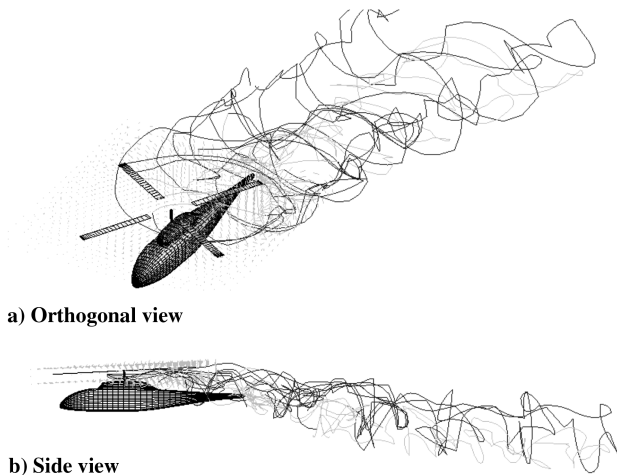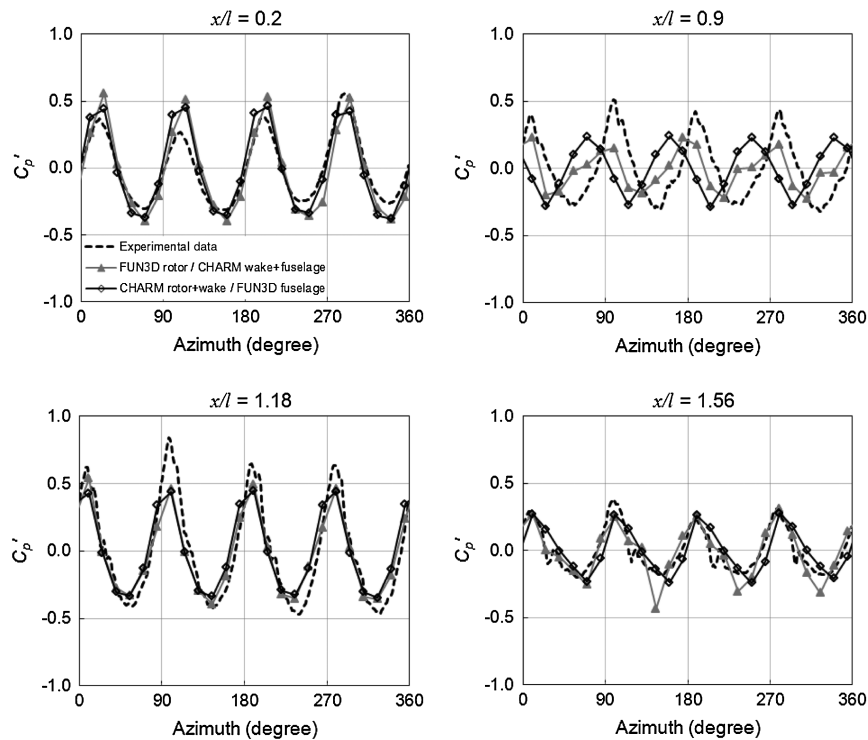
Fig. 4   Comparison of unsteady surface pressures along the top centerline of the ROBIN fuselage predicted with hybrid FUN3D/CHARM methods.

2.   CHARM Rotor Blades and Wake with FUN3D Fuselage

A new approach to the resolution of rotor–fuselage interactions is obtained when FUN3D and CHARM are coupled together in an open-loop manner such that the CHARM rotor and wake drives the solution on a viscous FUN3D fuselage. Periodic rotor airloads were precalculated with CHARM at 1 deg increments and used to set the outer boundary conditions on the FUN3D domain. At this point, the contribution of the unsteady $\partial \phi / \partial t$ term to the airloads was also calculated, where $\partial \phi / \partial t$ is the change in velocity potential over time in the unsteady Bernoulli equation. This contribution is added to the CFD fuselage loads during postprocessing. The FUN3D ROBIN

fuselage grid comprised 4.3 million cells with outer extents of one fuselage length in the freestream velocity directions, 0.5 lengths in width, and one length below the fuselage. The fuselage was oriented near the top of the grid so that the rotor disk plane was just above the upper computational domain boundary. Grid spacings were identical to the reference FUN3D simulation in [13], and the strut in the experiment was not modeled.

Wake predictions for this case are shown in Fig. 5, with CHARM vortex trailers on top of FUN3D vorticity isosurfaces. The rotor wake clearly descends below the rotor disk plane and smoothly enters the CFD domain before impacting the aft fuselage. Complicated rollup
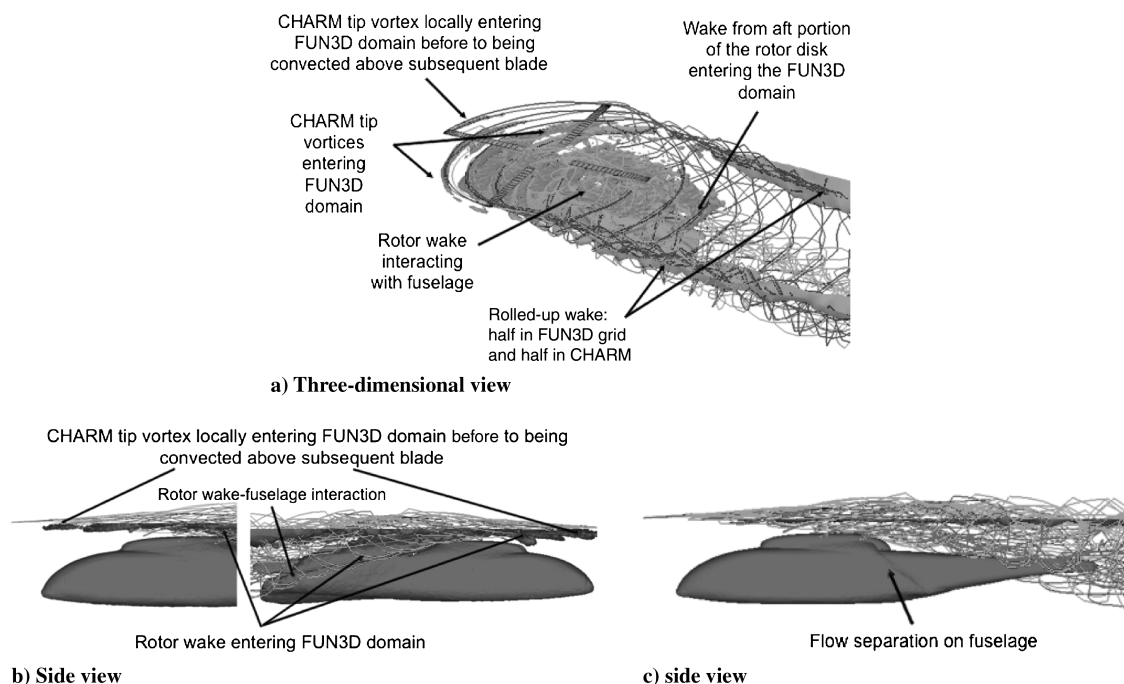

a) Three-dimensional view

b) Side view   c) side view

Fig. 5   Views of the hybrid FUN3D/CHARM ROBIN predictions (CHARM rotor and wake coupled to a FUN3D fuselage).

dynamics are observed near to the leading edge of the rotor where the tip vortices descend below the rotor disk and enter the CFD domain, before completing rollup and convecting upward to pass over the advancing blade. Aft of the rotor disk, the wake from each blade rolls up to form the supervortices, as illustrated in Fig. 5a. On the retreating side of the rotor, these vortices are observed to skim the upper boundary of the CFD domain, with half of the structure inside CFD domain and half being modeled solely by the free-wake solver, clearly demonstrating the efficacy of the coupling interface. On the advancing side of the rotor, the supervortices enter the CFD domain and pass close to the trailing edge of the fuselage. As noted previously, the tip vortices smoothly transition across the two numerical schemes; this is particularly evident upstream of the hub. Aft of the hub, complicated wake interactions occur where the inboard rotor wake impacts the rear of the fuselage.

Unsteady pressures along the centerline of the upper fuselage are plotted in Fig. 4. At $x/\ell = 0.9$, the pressure peaks are shifted by approximately 45 deg from the experiment and previous predictions, and this may be caused, at least in part, by the flow separation on the port side of the fuselage, shown in Fig. 5. However, the magnitude and phase of the pressure peaks are generally similar to the other hybrid approach and obtained with even greater reductions in computational cost. In addition, the suction peaks at 150 and 330 deg at $x/\ell = 1.56$ are better captured. Improvements to the slope predictions before the compression peaks at $x/\ell = 1.18$ can also be seen near 90 and 270 deg.

The hybrid results were obtained with significant reduction in computational costs compared with full CFD-alone simulations, requiring only 1.4 h per revolution compared with 17.1. Reductions in computational expense are achieved by 1) running a static CFD simulation without overset grids, and 2) reducing the extent of the CFD domain. The cost of running CHARM was less than 1 CPU hour per revolution, and the total cost of the hybrid simulation for seven revolutions was 630 CPU hours (compared with 3260 with FUN3D alone).

IV.   Conclusions

Two approaches to the application of a hybrid RANS CFD and free-wake methodology for rotor fuselage interactions have been demonstrated and assessed in their ability to predict the wake structure and unsteady fuselage pressures. The following conclusions can be stated from this effort:

1) The first ever hybrid calculations including a fuselage were performed, incorporating both an integral panel model and a CFD representation of the fuselage.

2) Computational cost of the free-wake-driven CFD hybrid approach is almost an order of magnitude less than the cost of a full CFD simulation with a moderately sized overset grid.

3) The different hybrid methodologies reveal the strength of the different computational approaches at various locations in the flow. On the top of the doghouse ($x/\ell = 0.9$), the conventional hybrid approach gives a better prediction of the pressure peaks due to viscous interactions near the rotor. Downstream of the doghouse ($x/\ell = 1.56$), the CHARM vortex trajectories coupled with the FUN3D viscous fuselage better capture the wake–fuselage interaction.

References

[1] Leishman, J. G., *Principles of Helicopter Aerodynamics*, Cambridge Univ. Press, New York, 2006, pp. 677.

[2] Komerath, N., Smith, M. J., and Tung, C., "A Review of Rotor Wake Physics and Modeling," *Journal of the American Helicopter Society*, Vol. 56, No. 2, pp. 1–19.
doi:10.4050/JAHS.56.022006

[3] Wissink, A., Potsdam, M., Sankaran, V., Sitaraman, J., Yang, Z., and Mavriplis, D. J., "A Coupled Unstructured-Adaptive Cartesian CFD Approach for Hover Prediction," *Proceedings of the 66th Annual Forum of the American Helicopter Society*, Phoenix, AZ, American Helicopter Soc., Alexandria, VA, May 2010.

[4] Shenoy, R., and Smith, M. J., "Unstructured Overset Grid Adaptation for Rotorcraft Aerodynamic Interactions," *Proceedings of the 67th Annual Forum of the American Helicopter Society*, Virginia Beach, VA, American Helicopter Soc., Alexandria, VA, May 2011.

[5] Wachspress, D. A., Quackenbush, T. R., and Boschitsch, A. H., "Rotorcraft Interactional Aerodynamics with Fast Vortex/Fast Panel Methods," *Journal of the American Helicopter Society*, Vol. 48, No. 4, 2003, pp. 1–13.
doi:10.4050/JAHS.48.223

[6] Anderson, W., and Bonhaus, D., "An Implicit Upwind Algorithm for Computing Turbulent Flows on Unstructured Grids," *Computers and Fluids*, Vol. 23, No. 1, 1994, pp. 1–21.
doi:10.1016/0045-7930(94)90023-X

[7] Quon, E., Smith, M. J., Whitehouse, G., and Wachspress, D., "Hierarchical Variable Fidelity Methods for Rotorcraft Aerodynamic Design and Analysis," *Proceedings of the 67th American Helicopter Society*, Virginia Beach, VA, American Helicopter Soc., Alexandria, VA, May 2–5, 2011.

[8] Whitehouse, G., and Tadghighi, H., "Investigation of Hybrid Grid-Based CFD Methods for Rotorcraft Flow Analysis," *Journal of the American Helicopter Society*, Vol. 56, No. 3, 2011, pp. 1–10.
doi:10.4050/JAHS.56.032000

[9] Quon, E., Smith, M. J., and Whitehouse, G., "Investigation of Boundary Conditions for Hybrid CFD," "*Journal of the American Helicopter Society*" (submitted for publication).

[10] Elliot, J. W., Althoff, S. L., and Sailey, R. H., "Inflow Measurements Made with a Laser Velocimeter on a Helicopter Model in Forward Flight. Volume I: Rectangular Planform Blades at an Advance Ratio of 0.15," NASA TM-100541, 1988.

[11] Mineck, R. E., and Althoff Gorton, S. L., "Steady and Periodic Pressure Measurements on a Generic Helicopter Fuselage Model in the Presence of a Rotor," NASA TM-2000-210286, 2000.

[12] Freeman, C. E., and Mineck, R. E., "Fuselage Surface Pressure Measurements of a Helicopter Wind-Tunnel Model with a 3.15-Meter Diameter Single Rotor," NASA TM-80051, 1979.

[13] Smith, M. J., Shenoy, R., Kenyon, A. K., and Brown, R. E., "Vorticity Transport and Unstructured RANS Investigation of rotor–fuselage Interactions," *Proceedings of the 35th European Rotorcraft Forum*, Hamburg, Germany, Deutsche Gesellschaft fuer Luft und Raumfahrt, Bonn, Sept. 2009.

[14] Kenyon, A. R., and Brown, R. E., "Wake Dynamics and Rotor: Fuselage Aerodynamic Interactions," *Journal of the American Helicopter Society*, Vol. 54, No. 1, 2009, pp. 1–18.
doi:10.4050/JAHS.54.012003